MITSUBISHI ELECTRIC RESEARCH LABORATORIES
https://www.merl.com

Backhaul Reliability Analysis on Cluster-Based Transmit Diversity Schemes in Private Networks

Kim, Kyeong Jin; Liu, Hongwu; Yeoh, Phee Lep; Orlik, Philip V.; Poor, H. Vincent

TR2020-170 December 16, 2020

Abstract

For a multi-cluster-based transmit diversity scheme that supports joint transmissions (JT) in private networks, a distributed remote radio unit system (dRRUS) is deployed in each of the clusters to increase the spectral efficiency and coverage, and to achieve flexible spatial degrees of freedom. Due to its distributed structure, the dRRUS relies on backhaul communications between the private network server (PNS) and cluster master (CM), which is the main backhaul communication, and between the CM to remote radio units (RRUs), which is the secondary backhaul communication. Thus, this paper mainly investigates the reliability of main and secondary backhaul connections for cluster-based transmit diversity schemes in private networks. Employing a Bernoulli process to model each backhaul reliability, a composite backhaul connection is modeled by an independent product of Bernoulli processes. By employing the distributed cyclic delay diversity scheme over the dRRUS and precision time protocol for clock synchronization, the multicluster-based JT can be achieved without full channel state information of the private network environment at the PNS and CMs. Having developed necessary distributions for the signal-tonoise ratio realized at the receiver, the closed-form expressions for the outage probability and spectral efficiency are derived. To verify their accuracy, the analytical performances are compared with link-level simulations.

IEEE Global Communications Conference (GLOBECOM)

Mitsubishi Electric Research Laboratories, Inc.
201 Broadway, Cambridge, Massachusetts 02139

Backhaul Reliability Analysis on Cluster-Based Transmit Diversity Schemes in Private Networks

Kyeong Jin Kim, Hongwu Liu, Phee Lep Yeoh, Philip V. Orlik, and H. Vincent Poor

***Abstract*—For a multi-cluster-based transmit diversity scheme that supports joint transmissions (JT) in private networks, a distributed remote radio unit system (dRRUS) is deployed in each of the clusters to increase the spectral efficiency and coverage, and to achieve flexible spatial degrees of freedom. Due to its distributed structure, the dRRUS relies on backhaul communications between the private network server (PNS) and cluster master (CM), which is the main backhaul communication, and between the CM to remote radio units (RRUs), which is the secondary backhaul communication. Thus, this paper mainly investigates the reliability of main and secondary backhaul connections for cluster-based transmit diversity schemes in private networks. Employing a Bernoulli process to model each backhaul reliability, a composite backhaul connection is modeled by an independent product of Bernoulli processes. By employing the distributed cyclic delay diversity scheme over the dRRUS and precision time protocol for clock synchronization, the multi-cluster-based JT can be achieved without full channel state information of the private network environment at the PNS and CMs. Having developed necessary distributions for the signal-to-noise ratio realized at the receiver, the closed-form expressions for the outage probability and spectral efficiency are derived. To verify their accuracy, the analytical performances are compared with link-level simulations.**

***Index Terms*—Private 5G networks, carrier aggregation, distributed cyclic delay diversity, joint transmission, backhaul reliability, diversity gain.**

I. Introduction

A private network is a promising new connectivity model enabling previously unavailable wireless network performance to businesses and individuals. The owners can guarantee coverage at their facility or location by planning and installing their own networks which satisfy individual security and privacy requirements. Since the owners have complete control over every aspect of the network, they can determine how resources are utilized, how traffic is prioritized, and how a specific security standard is deployed. Private networks will allow a wide range of industries, businesses, utilities, and public sectors to share in the benefits of 5G wireless networks with increasingly stringent performance requirements, in terms of availability, reliability, latency, device density, and throughput [1]. The deployment of private networks would be feasible in the licensed spectrum owned by operators, dedicated spectrum for private networks, and unlicensed spectrum. To increase transmission speeds, reduce latency, and boost the signal strength for the users, a dense deployment of small cells or clusters is expected [2].

To increase the spectral efficiency and coverage, a distributed antenna system (DAS) [3], [4], in which antennas are installed in a distributed manner over a coverage area of the base station (BS), is a promising approach for private networks. When each antenna operates as a BS, the DAS can be configured according to coordinated multiple point (CoMP) [5], [6] which supports simultaneous communications by a plurality of BSs to single or multiple users to improve the rate over a whole communication region. The CoMP approach includes coordinated beamforming and joint transmission (JT) as joint processing. However, this paper will focus on JT. Although the coordination between geographically separated BSs will require careful handling of path loss and shadowing [7], a major challenge is to collect full channel state information at the transmitter (CSIT) in the distributed system. Although a very reliable channel estimate can be obtained by the user, the feedback overhead will be overwhelming for large number of BSs increases.

In addition, a tight clock synchronization among BSs is required in JT. This is because a timing mismatch will cause interference at the user due to the difference in signal arrival times from all the BSs. It is noted that in the local area of private networks, for example, within factories and indoor environments, signals from Global Navigation Satellite System (GNSS) are usually not available. Thus, it is necessary to develop an alternative clock synchronization method.

With the proliferation of ultra-dense small cells, wireless backhauls are acquired to provide high speed data transportation from network nodes to end terminals and vice versa. Due to non-line-of-sight (nLoS) propagation, severe fading, and imperfect synchronization, the backhaul unreliability inherent from wireless impairments is a critical factor affecting the performance of wireless networks. In [8], mmWave communication was adopted in backhaul connections for 5G networks and the impact of nLoS propagation on backhaul reliability was investigated. For CoMP downlink cellular networks, the impacts of backhaul unreliability on the system performance were investigated in [9]. For distributed maximal ratio transmission (dMRT) [10], backhaul reliability was analyzed using the Bernoulli process. Since then, this model has been em-

K. J. Kim and P. V. Orlik are with Mitsubishi Electric Research Laboratories (MERL), Cambridge, MA 02139 USA

H. Liu is with Shandong Jiaotong University, Jinan, China

P. L. Yeoh is with The University of Sydney, NSW 2006 Australia.

H. V. Poor is with the Department of Electrical Engineering, Princeton University, Princeton, NJ 08544 USA

This work was supported in part by the U.S. National Science Foundation under Grant CCF-0939370

ployed in various systems such as for physical layer security [11] and spectrum sharing.

In this paper, we will investigate the following three problems.

- Pr_1: Since the distance between each of the remote radio units (RRUs) varies with respect to the receiver (RX), a key problem is that the received symbol timing cannot be aligned at the RX due to a path dependent propagation delay [12]. We assume that each RRU has only a single antenna and fixed transmit power for simple processing, so that a system comprising a plurality of RRUs, called the distributed remote radio unit system (dRRUS), is similar to a DAS [13], [14].
- Pr_2: CSIT-dependent precoders are usually employed to minimize interference caused by simultaneous multiple transmissions. Thus, the second problem is how to apply an interference-free transmission scheme to achieve transmit diversity.
- Pr_3: Backhaul communications are required in dRRUS, thus the third problem is how to investigate the impact of the reliability on performance in the private networks.

Taking into consideration Pr_1-Pr_3, we can summarize the following four contributions in this paper that advances previous work.

- C_1: A new multi-cluster-based distributed remote radio unit system (MC-dRRUS): To provide a greater throughput for the private network, we propose a new MC-dRRUS with carrier aggregation (CA), in which the private network server (PNS) provides transmission signals and synchronization to the respective cluster masters (CMs). Within non-overlapping clusters over different carriers, each CM forms a single dRRUS.
- C_2: A two-way packet exchange for clock synchronization: To make clock synchronization in the respective dRRUS, we adopt precision time protocol (PTP) [15], which provides a distribute method for transporting clock synchronization. The PNS works as the grandmaster clock, so that the private network will be synchronized to the PNS. By means of PTP, the CM and RRUs work as the boundary clock and transparent clocks, which have multiple ports to interact with other clocks. Thus, the PNS is able to estimate propagation delay without requiring feedback from the RX.
- C_3: Cyclic-prefixed single carrier (CP-SC) transmissions: To deal with frequency selective fading that is common in private networks, CP-SC transmissions are employed in the whole system.
- C_4: Distributed cyclic delay diversity-based JT (dCDD-JT) scheme: When the RRUs are clock synchronized to the PNS via its CM, and a distribution of propagation delays from RRUs to the RX is bounded by the cyclic prefix (CP) duration, the CM can achieve a synchronous dCDD for JT, which is possible by removing intersymbol interference (ISI) free signal reception at the RX.

Notation: $\boldsymbol{I}_N$ denotes an $N \times N$ identity matrix; $\mathbf{0}$ denotes an all-zero matrix of with an appropriate size; and $\mathcal{CN}\left(\mu, \sigma^2\right)$ denotes a complex Gaussian distribution with mean μ and variance σ^2. The binomial coefficient is denoted by $\binom{n}{k} \triangleq \frac{n!}{(n-k)!k!}$. For a vector $\boldsymbol{a}$, $\mathbb{L}(\boldsymbol{a})$ denotes the cardinality; and its lth element is denoted by $\boldsymbol{a}(l)$.

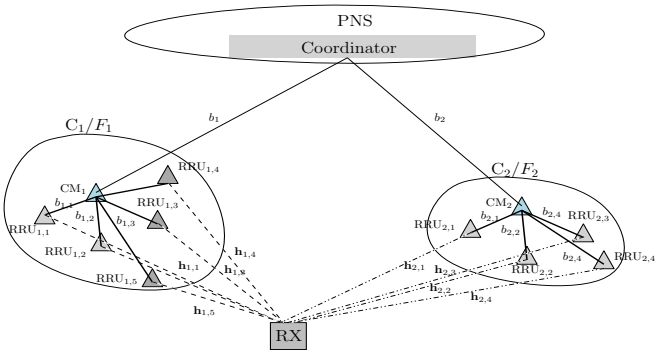

Fig. 1. Illustration of the proposed multi-cluster-dRRUS, where a PNS coordinator transmits to the RX user via five RRUs in C_1 and four RRUs in C_2. Two nodes highlighted in blue are assigned as CMs to control the RRUs in its cluster.

II. System and Channel Models

Fig. 1 illustrates the considered MC-dRRUS with two non-overlapping and co-located clusters. Each cluster is considered to be an individual dRRUS. Owing to CA, the second cluster C_2 is deployed in a different carrier from that of the first cluster C_1. The PNS works as the grand master clock by PTP, so that each CM and RRU can achieve clock synchronization with respect to the PNS. Non-ideal backhaul links, $\{b_1, b_2\}$, are configured to provide the main backhaul communication links to the clusters via the coordinator that resides at the PNS. The secondary backhaul communication links, $\{b_{i,j}, i = 1, 2, j = 1, \ldots, K\}$, provide non-ideal backhaul access to RRUs via the CM. The CM controls all RRUs and is responsible for transmitting the signals. All nodes in the cluster are assumed to be equipped with a single antenna.

A frequency selective fading channel from the kth RRU, deployed in the ith cluster, to the RX is denoted by $\boldsymbol{h}_{i,k}$ with $\mathbb{L}(\boldsymbol{h}_{i,k}) = N_{i,k}$. The distance-dependent large scaling fading is denoted by $\alpha_{i,k}$. For a distance $d_{i,k}$ from $\mathrm{RRU}_{i,k}$ to the RX, $\alpha_{i,k}$ is defined by $\alpha_{i,k} = (d_{i,k})^{-\epsilon}$, where ϵ denotes the path loss exponent. The RX is placed at a specific location with respect to the RRUs, and, thus, independent but non-identically distributed (i.n.i.d.) frequency selective fading channels from the RRUs to RX are considered in the dRRUS. The RX is assumed to have knowledge of the number of multipath components of the channels connected to itself by either sending a training sequence or adding a pilot as the suffix to each symbol block. To reduce the feedback overhead, the RX first computes $N_{\max} \triangleq \max\{N_{i,k}, \forall i, k\}$, and then feeds back $N_{\max}$ to the PNS, so that it is not necessary for the CMs to use the X2 interface to exchange their channel relevant parameters.

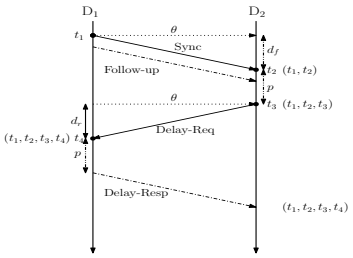

Fig. 2. Two-way packet exchange for synchronization. A filled circle dot denotes a timestamp in the event message recorded at its transmission and reception. The processing time taken at all the nodes is assumed to be p.

To estimate the clock offset, θ, and propagation delay, d, the PTP [15] specifies four event messages, known as Sync, Delay-Req, Pdelay-Req, and Pdelay-Resp, within which an accurate hardware timestamp is generated and recorded at transmission and reception of its respective messages. Thus, after exchanging two-way packets between D_1 and D_2, four hardware timestamps, (t_1, t_2, t_3, t_4), are available at D_1 and D_2. Based on the four timestamps, d and θ are respectively computed as follows:

$$d \approx \frac{(t_4 + t_2) - (t_3 + t_1)}{2} \text{ and } \theta \approx \frac{(t_3 - t_1) - (t_4 - t_2)}{2} \quad (1)$$

where we have assumed that the forward propagation delay, d_f, is almost equal to the backward propagation delay, d_r, i.e., $d_f \approx d_r$. Applying the same procedure, D_1 can estimate propagation delay to another node, D_3, which supports PTP, so that it can be synchronized to D_2.

The distributed CDD (dCDD) scheme was proposed by [13] for distributed CP-SC transmissions to achieve transmit diversity without requiring full CSIT. Depending on the block size, Q, of the transmission symbol, $\boldsymbol{s} \in \mathbb{C}^{Q\times 1}$, and the cyclic-prefix (CP) length, $N_{\rm CP}$ which is set to $N_{\max}$, the maximum number of RRUs that can achieve ISI-free reception at the RX is determined by $M = \lfloor Q/N_{\rm CP} \rfloor$, where $\lfloor \cdot \rfloor$ denotes the floor function. When the ith dRRUS is underpopulated[1], i.e., $K_i \leq M$, the CDD delay for the kth RRU is assigned as follows:

$$\Delta_k = (k-1)N_{\rm CP},\ k = 1, \ldots, K \quad (2)$$

Thus, for underpopulated dRRUSs, only partial CSIT, $N_{\rm CP}$, is required at the PNS, which can be obtained from each CM_i via the main backhaul communications. This means that dRRUSs can perform the same objective as dMRT. If one CDD delay, Δ_k, is exclusively assigned to one RRU, $\mathrm{RRU}_{i,k}$, with $k \neq \tilde{k}$, then the same performance can be achieved as that of main backhaul scenario to a single CM that was analyzed by [13]. Thus, (2) can be recognized as a linear CDD assignment.

III. dCDD-JT for CP-SC Transmissions

After the removal of the CP signal, the RX receives a composite signal from two clusters given by

$$\boldsymbol{r} = \sum\nolimits_{k=1}^{K} \Big[\big[\sqrt{P_T \alpha_{1,k}} \mathbb{I}_{1,k} \boldsymbol{H}_{1,k} [\boldsymbol{P}_{1,k} \boldsymbol{s}]_{J_3} \big]_{J_1} + \big[\sqrt{P_T \alpha_{2,k}} \mathbb{I}_{2,k} \boldsymbol{H}_{2,k} [\boldsymbol{P}_{2,k} \boldsymbol{s}]_{J_4} \big]_{J_2} \Big] + \boldsymbol{z} \quad (3)$$

[1]Overpopulated dRRUS with $K > M$, will be considered in our future work.

where P_T denotes the transmission power for single carrier transmissions. In addition, $\mathbb{I}_{j,k}$ models reliability of the kth secondary backhaul, $b_{j,k}$, within cluster C_j, via the jth main backhaul, b_j. When the backhaul reliability is modeled by a Bernoulli process, that is, $Pr(b_j = 1) = p_j$, $Pr(b_j = 0) = 1 - p_j$ and $Pr(b_{j,k} = 1) = p_{j,k}$, $Pr(b_{j,k} = 0) = 1 - p_{j,k}$, then we can specify a Bernoulli process $\mathbb{I}_{j,k}$ with $Pr(\mathbb{I}_{j,k} = 1) = p_j p_{j,k} \triangleq R_{j,k}$ and $Pr(\mathbb{I}_{j,k} = 0) = 1 - R_{j,k}$. The two terms labeled by $[\cdot]_{J_1}$ and $[\cdot]_{J_2}$ respectively represent signals transmitted from C_1 and C_2. Note that due to the deployment of the MC-dRRUS with CA, C_1 is assumed to be operating at carrier frequency F_1, whereas C_2 is assumed to be operating at carrier frequency F_2 with $F_1 \neq F_2$. In addition, $\boldsymbol{H}_{i,k}$ is right circulant matrix determined by $\boldsymbol{h}_{i,k}$. Since full CSIT is not available in the considered system, the same P_T is assigned to all the RRUs. The additive vector noise is denoted by $\boldsymbol{z} \sim \mathcal{C}N(\boldsymbol{0}, \sigma_z^2 \boldsymbol{I}_Q)$. Furthermore, $[\cdot]_{J_3}$ and $[\cdot]_{J_4}$ correspond to local signal processing operations respectively performed at $\mathrm{RRU}_{1,m}$ and $\mathrm{RRU}_{2,m}$. To make ISI-free reception at the RX, it is required that $\boldsymbol{P}_{1,m}$ and $\boldsymbol{P}_{2,m}$ are orthogonal and right circulant matrices, and meet the CDD delay assignment for $\mathrm{RRU}_{i,m}$. By circularly shifting down the transmission symbol $\boldsymbol{s}$ by Δ_k in (2), operation J_3 can be simply accomplished. Similar operation is conducted for J_4. Thus, $\boldsymbol{P}_{1,k}$ and $\boldsymbol{P}_{2,k}$ can be obtained from $\boldsymbol{I}_Q$ by circularly shifting down respectively by Δ_k.

IV. Performance Analysis of MC-dCDD-based JT

Using the properties of the right circulant matrix, the achievable signal-to-noise ratio (SNR) realized by MC-dCDD based JT can be derived by the following *Theorem 1*.

Theorem 1: Based on the proposed MC-dCDD, ISI-free reception can be achieved at the RX. Thus, the achievable SNR realized by JT is given by

$$\gamma_{\rm JT} = \rho \big(\sum\nolimits_{k=1}^{K} \mathbb{I}_{1,k} \alpha_{1,k} \|\boldsymbol{h}_{1,k}\|^2 + \sum\nolimits_{k=1}^{K} \mathbb{I}_{2,k} \alpha_{2,k} \|\boldsymbol{h}_{2,k}\|^2 \big) = \gamma_{\rm JT,1} + \gamma_{\rm JT,2} = \rho_s / \sigma_z^2 \quad (4)$$

where $\rho_s = P_T \big(\sum_{k=1}^{K} \mathbb{I}_{1,k} \alpha_{1,k} \|\boldsymbol{h}_{1,k}\|^2 + \sum_{k=1}^{K} \mathbb{I}_{2,k} \alpha_{2,k} \|\boldsymbol{h}_{2,k}\|^2 \big)$ and $\gamma_{{\rm JT},i} \triangleq \rho \sum_{k=1}^{K} \mathbb{I}_{i,k} \alpha_{i,k} \|\boldsymbol{h}_{i,k}\|^2$ with $\rho \triangleq P_T / \sigma_z^2$.

Proof: When $\{\boldsymbol{h}_{1,k}, \forall k\}$ and $\{\boldsymbol{h}_{2,k}, \forall k\}$ are independent of each other, ρ_s, realized at the RX, is determined by the summation of their squared Euclidean norms. ■

Theorem 1 proves that by compensating different signal arrival times at the RX, the MC-dCDD makes JT provide the same benefit as dMRT without full CSIT at the PNS and CMs.

Theorem 2: Due to the use of dCDD based JT, the proposed MC-dRRUS results in the SNR, $\gamma_{\rm JT}$ realized at the RX, whose moment generating function (MGF) is given by

$$M_{\gamma_{\rm JT}}(s) = \widetilde{\sum_{l_1}} \widetilde{\sum_{l_2}} \prod\nolimits_{j=1}^{2K} (s + \tilde{\beta}_j)^{-l_j N_j} \quad (5)$$

where $\tilde{\beta}_j$, l_j, and N_j respectively denote the jth elements of $\tilde{\boldsymbol{\beta}} = [1/\tilde{\alpha}_{1,1}, \ldots, 1/\tilde{\alpha}_{1,K}, 1/\tilde{\alpha}_{2,1}, \ldots, 1/\tilde{\alpha}_{2,K}]^T$,

$\boldsymbol{l} = [l_{1,1}, \ldots, l_{1,K}, l_{2,1}, \ldots, l_{2,K}]^T$, and $\boldsymbol{N} = [N_{1,1}, \ldots, N_{1,K}, N_{2,1}, \ldots, N_{2,K}]^T$. Additional terms specified in (5) are defined in Appendix A.

Proof: See Appendix A. ∎

In general, as either K or $N_{\max}$ increases, the inverse MGF (IMGF) based on the partial fraction (PF) becomes unreliable, thus it is necessary to develop a reliable approximation of Theorem 2, which is provided in the following corollary.

Corollary 1: An accurate and reliable approximation of the MGF in (5) is given by

$$M_{\gamma_{\mathrm{JT}}}(s) = \widetilde{\sum_{l_1}} \widetilde{\sum_{l_2}} \sum_{l=0}^{N_1} \delta_l (b_I)^{-l} (1/b_I + s)^{-G_d - l} \quad (6)$$

where $G_d \triangleq \sum_{j=1}^{2K} N_j$, $b_I \triangleq \min(1/\tilde{\beta}_1, \ldots, 1/\tilde{\beta}_{2K})$, N_1 denotes an upper limit summation, and $\delta_l \triangleq \frac{1}{l} \sum_{i=1}^{l} i r_i \delta_{l-i}$ with $\delta_0 = 1$ and $r_i = \sum_{j=1}^{2K} N_j (1 - b_I \tilde{\beta}_i)^j$.

Proof: See [16]. ∎

Corollary 1 provides the MGF expressed by the weighted sum of $N_1 + 1$ terms, proportional to $(1/b_I + s)^{-G_d - l}$. Thus, the following corollary can be immediately derived.

Corollary 2: The CDF of γ_{JT} can be expressed by a finite number of gamma distributions.

$$F_{\gamma_{\mathrm{JT}}}(x) = 1 - \widetilde{\sum_{l_1}} \widetilde{\sum_{l_2}} \sum_{l=0}^{N_1} \delta_l (b_I)^{-l} ((b_I)^{G_d + l} / \Gamma(G_d + l)) \Gamma_u(G_d + l, x/b_I) \quad (7)$$

where $\Gamma(\cdot)$ and $\Gamma_u(\cdot, \cdot)$ respectively denote complete gamma and incomplete upper-gamma functions.

Based on (7), the outage probability and spectral efficiency of the proposed MC-dCDD based JT are derived.

A. Outage Probability

Since the closed-form expression for the CDF is derived in (7), the outage probability can be readily obtained as

$$\mathrm{OP} = F_{\gamma_{\mathrm{JT}}}(o_{\mathrm{th}}) \quad (8)$$

where o_{th} is the SNR threshold below which an outage event occurs in the dRRUS.

B. Spectral Efficiency

Theorem 3: The achievable spectral efficiency of the proposed JT realized by MC-dCDD is given by

$$\mathrm{SE} = \frac{1}{\log(2)} \widetilde{\sum_{l_1}} \widetilde{\sum_{l_2}} (b_I)^{G_d} \left[\sum_{l=0}^{N_1} \frac{\delta_l}{\Gamma(G_d + l)} G_{2,3}^{3,1}\left(1/b_I \middle| \begin{matrix} 0, 1 \\ G_d + l, 0, 0 \end{matrix}\right) \right] \quad (9)$$

where $G_{p,q}^{m,n}\left(t \middle| \begin{matrix} a_1, \ldots, a_n, a_{n+1}, \ldots, a_p \\ b_1, \ldots, b_m, b_{m+1}, \ldots, b_q \end{matrix}\right)$ denotes the Meijer G-function [17, Eq. (9.301)].

Proof: We first express the functions of x in terms of Meijer G-functions, i.e., $(1 + x)^{-1} = G_{1,1}^{1,1}\left(x \middle| \begin{matrix} 0 \\ 0 \end{matrix}\right)$ and $\Gamma_u(j, \alpha x) = G_{1,2}^{2,0}\left(\alpha x \middle| \begin{matrix} 1 \\ j, 0 \end{matrix}\right)$. After this, applying [18, eq. (2.24.1,2)], we can derive (9). ∎

C. Diversity Gain Analysis

Depending on the noise power, we can distinguish the operating regions into the noise dominant cooperative region at low SNRs and the backhaul reliability dominant regions at high SNRs. Specifically, we find that when the SNR increases, the proposed MC-dRRUS will leave the cooperative region, and the diversity gain is not achievable.

Corollary 3: In the backhaul reliability dominant region, the asymptotic outage probability at high SNRs is given by

$$\mathrm{OP}^{\mathrm{as}} = \prod_{k=1}^{K} (1 - R_{1,k}) \prod_{k=1}^{K} (1 - R_{2,k}). \quad (10)$$

Proof: See Appendix B. ∎

Note that this is a similar observation that was analyzed in [10]. In contrast, in the cooperative region at low SNRs, a transmit diversity gain can be achievable via JT.

V. Simulation Results

We assume the following simulation setup.

1) C_1: Six RRUs are placed at $(-1.2, 4.7)$, $(0.7, 4.0)$, $(3.0, 3.0)$, $(-2.5, 2.7)$, $(-3.3, 0.4)$, and $(-3.0, 3.5)$. The first cluster master, CM_1, is placed at $(0, 2)$ in a 2-D plane.
2) C_2: Four RRUs are placed at $(12.8, 3.3)$, $(7.4, 2.5)$, $(10.0, 4.6)$, and $(9.0, 1.7)$. The second cluster master, CM_2, is placed at $(10.0, 3.0)$ in a 2-D plane.
3) For CP-SC transmissions, we assume that $Q = 64$ and $N_{\mathrm{CP}} = 8$. Thus, the CMs can support up to eight RRUs for dCDD operation, i.e., $M = 8$.
4) RX is placed at $(3, -3)$.
5) In all scenarios, we fix $P_T = 1$. A fixed path-loss exponent is assumed to be $\epsilon = 2.09$.

We consider several frequency selective fading channel parameters shown below for two clusters depending on the respective number of RRUs, K_1 and K_2. For notation purposes, we use $\mathcal{H}_1 = \{N_{1,j}, j = 1, \ldots, K_1\}$ for C_1 and $\mathcal{H}_2 = \{N_{2,j}, j = 1, \ldots, K_2\}$ for C_2. Reliability of the main backhauls b_1 and b_2 is assumed to be 0.99.

1) $\mathcal{X}_1$: $\mathcal{H}_1 = \{2, 3, 4, 2\}$ with $R_{1,k} = \{0.9, 0.95, 0.94, 0.8\}$ and $\mathcal{H}_2 = \{3, 2, 3\}$ with $R_{2,k} = \{0.88, 0.96, 0.97\}$.
2) $\mathcal{X}_2$: $\mathcal{H}_1 = \{2, 3, 2, 2\}$ with $R_{1,k} = \{0.9, 0.95, 0.94, 0.8\}$ and $\mathcal{H}_2 = \{3, 2, 3\}$ with $R_{2,k} = \{0.88, 0.96, 0.97\}$.
3) $\mathcal{X}_3$: $\mathcal{H}_1 = \{2, 3, 4\}$ with $R_{1,k} = \{0.9, 0.95, 0.94\}$ and $\mathcal{H}_2 = \{3, 2, 3\}$ with $R_{2,k} = \{0.88, 0.96, 0.97\}$.
4) $\mathcal{X}_4$: $\mathcal{H}_1 = \{2, 3, 4, 3\}$ with $R_{1,k} = \{0.9, 0.95, 0.94, 0.8\}$ and $\mathcal{H}_2 = \{3, 2, 3, 4\}$ with $R_{2,k} = \{0.88, 0.96, 0.97\}$.

We denote the analytically derived performance metric by **An**, whereas we denote the exact performance metric obtained by the link-level simulations by **Ex** in the sequel.

A. Outage probability analysis

From Fig. 3, we first verify the analytically derived outage probabilities for various numbers of RRUs and channel parameters. The figure shows that the analytically derived outage probabilities match closely with the exact link-level

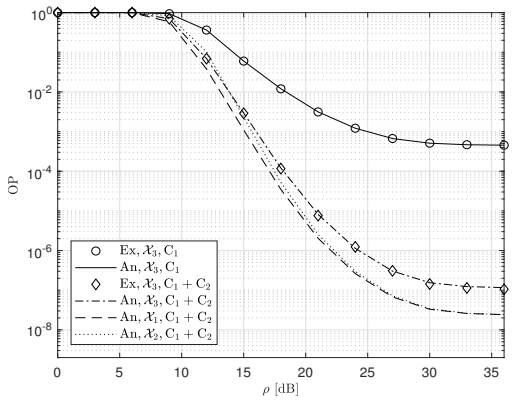

Fig. 3. Outage probability for various system and channel parameters.

simulations. This figure also shows that if N_1 is sufficiently large, the outage approximation proposed by *Corollary 1*, reliably approximates the simulation results. For scenario $\mathcal{X}_3$, we compare the outage probability of the dRRUS with two clusters with that of a single cluster. The figure shows that CA between the two clusters results in a lower outage probability for dCDD-JT in cooperative and backhaul reliability dominant regions.

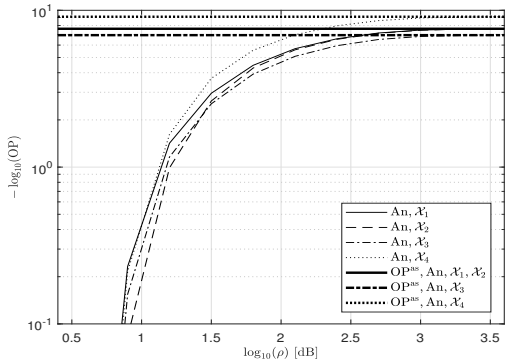

Fig. 4. Outage probability for various scenarios.

In Fig. 4, we plot the outage probability in terms of $-\log_{10}(\mathrm{OP})$ to investigate the impact of backhaul reliability on the asymptotic outage probability at high SNRs. We also plot the asymptotic lower bound on the outage probability. From Figs. 3 and 4, we can extract the following facts:

- As the dRRUS is populated with more RRUs, a lower outage probability can be achieved.
- As the number of clusters increases, a lower outage probability can be achieved.
- Diversity gain can be observed only in the cooperative region. As the SNR increases, MC-dRRUS leaves the cooperative region, so that backhaul reliability tends to determine the lower bound on the outage probability. However, in general, the outage probability still decreases as the number of clusters increases.

At 15 dB SNR, Fig. 5 shows the impact of improving the reliability of the main backhaul, b_1, on the outage probability.

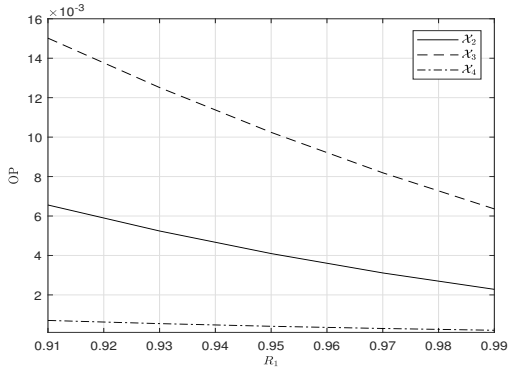

Fig. 5. Outage probability for various reliability of the main backhaul.

Other backhauls are assumed to have the same reliability as specified in the scenarios. The figure shows that the main backhaul exerts a stronger influence over less populated dRRUSs than on more populated dRRUSs.

B. Spectral efficiency analysis

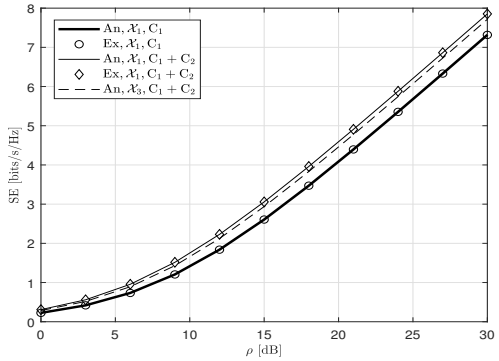

Fig. 6. Spectral efficiency for various system and channel parameters.

Fig. 6 shows the spectral efficiency for various system and channel parameters. From this figure we can observe the following facts:

- The approximate closed-form expression for the spectral efficiency provides a reliable spectral efficiency irrespective of the population of the dRRUS.
- As the number of clusters increases for the dRRUS, a greater spectral efficiency can be obtained. Especially, at 15 dB SNR, the use of two clusters for scenario $\mathcal{X}_1$ provides 0.5 bits/s/Hz greater spectral efficiency than a single cluster.
- A greater population of each dRRUS results in a greater spectral efficiency.

VI. Conclusions

In this paper, we have investigated the backhaul reliability in a proposed multiple cluster-based transmit diversity scheme. We have shown that distributed systems composed of remote radio heads can relax the requirement of full channel state information at the private network server by employing the

distributed cyclic delay diversity scheme. We have also shown that backhaul reliability is a key constraint to maintain the target performance especially at high SNRs. For i.n.i.d. frequency selective fading channels, and non-identical backhaul reliability over main and secondary backhaul connections, new closed-form expressions for the outage probability and spectral efficiency have been derived. The accuracy of the derived analytical expressions have been also verified with their corresponding link-level simulations. Due to backhaul reliability, we have found that the MC-dRRUS displays two distinctive operating regions, namely, the cooperative region and the backhaul reliability dominant region. Their existence has been verified theoretically and numerically. We confirm that careful design of the MC-dRRUS to remain within the cooperative region, will result in reaping the transmit diversity gains of joint transmission without requiring full channel state information.

Appendix A: Proof of Theorem 2

To simplify the notation, let us define x_k as $x_k \triangleq \rho\alpha_{1,k}\mathbb{I}_{1,k}\|\boldsymbol{h}_{1,k}\|^2 \triangleq \tilde{\alpha}_{1,k}\mathbb{I}_{1,k}\|\boldsymbol{h}_{1,k}\|^2$. According to a Bernoulli process, the PDF of x_k is given by [10]

$$f_{x_k}(x) = (1-R_{1,k})\delta(x) + R_{1,k}\frac{e^{-x/\tilde{\alpha}_{1,k}}x^{N_{1,k}-1}}{\Gamma(N_{1,k})(\tilde{\alpha}_{1,k})^{N_{1,k}}} \quad \text{(A.1)}$$

where $\delta(x)$ denotes the Dirac delta function. Based on the PDF, the corresponding MGF is given by

$$\begin{aligned} M_{1,k}(s) &= (1-R_{1,k}) + \left(R_{1,k}/\tilde{\alpha}_{1,k}^{N_{1,k}}\right)(s+1/\tilde{\alpha}_{1,k})^{-N_{1,k}} \\ &= \sum_{l_{1k}=0}^{1}(1-R_{1,k})^{1-l_{1k}}\left(\frac{R_{1,k}}{\tilde{\alpha}_{1,k}^{N_{1,k}}}\right)^{l_{1k}}(s+1/\tilde{\alpha}_{1,k})^{-l_{1k}N_{1,k}} \quad \text{(A.2)} \end{aligned}$$

where the binomial theorem is used in the final expression. According to (A.2), the MGF of $\gamma_{\mathrm{JT},1}$ is given by

$$\begin{aligned} M_{\gamma_{\mathrm{JT},1}}(s) &= \sum_{l_{11}=0}^{1}\cdots\sum_{l_{1K}=0}^{1}\prod_{j=1}^{K}\left((1-R_{1,k})^{1-l_{1j}}\left(\frac{R_{1,j}}{\tilde{\alpha}_{1,j}^{N_{1,j}}}\right)^{l_{1j}}\right) \\ &\quad \prod_{j=1}^{K}(s+1/\tilde{\alpha}_{1,j})^{-l_{1j}N_{1,j}} \\ &= \widetilde{\sum_{l_1}}\prod_{j=1}^{K}(s+1/\tilde{\alpha}_{1,j})^{-l_{1j}N_{1,j}} \quad \text{(A.3)} \end{aligned}$$

where $\widetilde{\sum_{l_1}} \triangleq \sum_{l_{11}=0}^{1}\cdots\sum_{l_{1K}=0}^{1}\prod_{j=1}^{K}\left((1-R_{1,k})^{1-l_{1j}}(R_{1,j}/\tilde{\alpha}_{1,j}^{N_{1,j}})^{l_{1j}}\right)$.

With an assumption that K RRUs are selected by CM_2, the MGF of $\gamma_{\mathrm{JT},2}$ can be derived as follows:

$$M_{\gamma_{\mathrm{JT},2}}(s) = \widetilde{\sum_{l_2}}\prod_{j=1}^{K}(s+1/\tilde{\alpha}_{2,j})^{-l_{2j}N_{2,j}} \quad \text{(A.4)}$$

where $\widetilde{\sum_{l_2}} \triangleq \sum_{l_{21}=0}^{1}\cdots\sum_{l_{2K}=0}^{1}\prod_{j=1}^{K}\left((1-R_{2,k})^{1-l_{2j}}(R_{2,j}/\tilde{\alpha}_{2,j}^{N_{2,j}})^{l_{2j}}\right)$. Since the SNR realized at the RX is the sum of two RVs, $\gamma_{\mathrm{JT},1}$ and $\gamma_{\mathrm{JT},2}$, the MGF is given by

$$M_{\gamma_{\mathrm{JT}}}(s) = M_{\gamma_{\mathrm{JT},1}}(s)M_{\gamma_{\mathrm{JT},2}}(s). \quad \text{(A.5)}$$

Appendix B: Proof of Corollary 3

For the kth RRUs, we can compute

$$\begin{aligned} M_k(s) &= M_{1,k}(s)M_{1,k}(s) \\ &= \left((1-R_{1,k}) + \left(R_{1,k}/\tilde{\alpha}_{1,k}^{N_{1,k}}\right)(s+1/\tilde{\alpha}_{1,k})^{-N_{1,k}}\right) \\ &\quad \left((1-R_{2,k}) + \left(R_{2,k}/\tilde{\alpha}_{2,k}^{N_{2,k}}\right)(s+1/\tilde{\alpha}_{2,k})^{-N_{2,k}}\right). \quad \text{(B.1)} \end{aligned}$$

As the SNR increases, $M_k(s)$ is governed by $(1-R_{1,k})$, that is, at $l_{1k}=0$ and $l_{2k}=0$. Thus, $M_k(s) \overset{\rho\to\infty}{\approx} (1-R_{1,k})$. Eventually, $M(s) \overset{\rho\to\infty}{\approx} \prod_{k=1}^{K}(1-R_{1,k})\prod_{k=1}^{K}(1-R_{2,k})$.

References

[1] J. Mietzner, "A survey of resource management toward 5G radio access networks," *IEEE Commun. Surveys Tuts.*, vol. 18, no. 3, pp. 1656–1686, 2016.

[2] H. Li, J. Hajipour, A. Attar, and V. C. M. Leung, "Efficient HetNet implementation using broadband wireless access with fiber-connected massively distributed antennas architecture," *IEEE Wireless Commun.*, vol. 18, no. 3, pp. 72–78, Jun. 2011.

[3] X. Zhang *et al.*, "Distributed power allocation for coordinated multipoint transmissions in distributed antenna systems," *IEEE Trans. Wireless Commun.*, vol. 12, no. 5, pp. 2281–2291, May 2013.

[4] W. Feng, Y. Wang, N. Ge, J. Lu, and J. Zhang, "Virtual MIMO in multi-cell distributed antenna systems: Coordinated transmissions with large-scale CSIT," *IEEE J. Sel. Areas Commun.*, vol. 31, no. 10, pp. 2067–2081, Oct. 2013.

[5] X. Tao, X. Xu, and Q. Cui, "An overview of cooperative communications," *IEEE Commun. Mag.*, pp. 65–71, Jun. 2012.

[6] V. Garcia, Y. Zhou, and J. Shi, "Coordinated multipoint transmission in dense cellular networks with user-centric adaptive clustering," *IEEE Trans. Wireless Commun.*, vol. 13, no. 8, pp. 4297–4308, Aug. 2014.

[7] H. Zhuang, L. Dai, L. Xiao, and Y. Yao, "Spectral efficiency of distributed antenna system with random antenna layout," *Electronics Letters*, vol. 39, no. 6, pp. 495–496, Mar. 2003.

[8] H. Jung and I. H. Lee, "Outage analysis of millimeter-wave wireless backhaul in the presence of blockage," *IEEE Commun. Lett.*, vol. 20, no. 11, pp. 2268–2271, Nov. 2016.

[9] Z. Mayer, J. Li, A. Papadogiannis, and T. Svensson, "On the impact of control channel reliability on coordinated multi-point transmission," *EURASIP J. Wireless Commun. Netw.*, vol. 2014, no. 28, pp. 1–16, 2014.

[10] K. J. Kim, T. Khan, and P. Orlik, "Performance analysis of cooperative systems with unreliable backhauls and selection combining," *IEEE Trans. Veh. Technol.*, vol. 66, no. 3, pp. 2448–2461, Mar. 2017.

[11] K. J. Kim, P. L. Yeoh, P. Orlik, and H. V. Poor, "Secrecy performance of finite-sized cooperative single carrier systems with unreliable backhaul connections," *IEEE Trans. Signal Process.*, vol. 64, no. 17, pp. 4403–4416, Sep. 2016.

[12] H. Wang, "Full-diversity uncoordinated cooperative transmission for asynchronous relay networks," *IEEE Trans. Veh. Technol.*, vol. 66, no. 1, pp. 1939–9359, Jan. 2017.

[13] K. J. Kim, M. D. Renzo, H. Liu, P. V. Orlik, and H. V. Poor, "Performance analysis of distributed single carrier systems with distributed cyclic delay diversity," *IEEE Trans. Commun.*, vol. 65, no. 12, pp. 5514–5528, Dec. 2017.

[14] K. J. Kim, H. Liu, M. D. Renzo, P. V. Orlik, and H. V. Poor, "Secrecy analysis of distributed CDD-based cooperative systems with deliberate interference," *IEEE Trans. Wireless Commun.*, vol. 17, no. 12, pp. 7865–7878, Dec. 2018.

[15] A. Mahmood, R. Exel, H. Trsek, and T. Sauter, "Clock synchronization over IEEE 802.11–A survey of methodologies and protocols," *IEEE Trans. Ind. Informat.*, vol. 13, no. 2, pp. 907–922, Apr. 2017.

[16] P. G. Moschopoulos, "The distribution of the sum of independent gamma random variables," *Ann. Inst. Statist. Math. (PartA)*, vol. 37, pp. 541–544, 1985.

[17] I. S. Gradshteyn and I. M. Ryzhik, *Table of Integrals, Series, and Products*. New York: Academic Press, 2007.

[18] A. P. Prudnikov, Y. A. Brychkov, and O. I. Marichev, *Integral and Series. Vol. 3: More Special Functions*, 3rd ed. London: Gordon and Breach, 1992.